Received: 14 July 2017 | Revised: 11 September 2017 | Accepted: 11 September 2017

DOI: 10.1002/aoc.4128

FULL PAPER

WILEY Applied Organometallic Chemistry

New anthracene based Schiff base ligands appended Cu(II) complexes: Theoretical study, DNA binding and cleavage activities

Ammavasai Gubendran[1,2] | Gujuluva Gangatharan Vinoth Kumar[3] | Mookkandi Palsamy Kesavan[3] | Gurusamy Rajagopal[4] | Periakaruppan Athappan[1] | Jegathalaprathaban Rajesh[1,3]

[1] Department of Inorganic Chemistry, School of Chemistry, Madurai Kamaraj University, Madurai 625 021, Tamilnadu, India

[2] Department of Chemistry, Saraswathi Narayanan College, Madurai 625 022, Tamilnadu, India

[3] Chemistry Research Centre, Mohamed Sathak Engineering College, Kilakarai 623 806, Tamilnadu, India

[4] PG and Research Department of Chemistry, Chikkanna Government Arts College, Tiruppur 641 602, Tamilnadu, India

Correspondence
Dr. Jegathlaprathaban Rajesh, Associate Professor, Chemistry Research Centre, Mohamed Sathak Engineering College, Killakarai - 623 806, Ramanthapuram (District), Tamilnadu, India.
Email: mkuraji@gmail.com

Funding information
DST-SERB, Grant/Award Number: SB/FT/CS-130/2012

New anthracene based Schiff base ligands $\mathbf{L^1}$ and H($\mathbf{L^2}$), their Cu(II) complexes [Cu($\mathbf{L^1}$)Cl_2] (**1**) and [Cu($\mathbf{L^2}$)Cl] (**2**), (where $\mathbf{L^1}$ = N^1,N^2-*bis*(anthracene-9-methylene)benzene-1,2-diamine, $\mathbf{L^2}$ = (2*Z*,4*E*)-4-(2-(anthracen-9-ylmethyleneamino) phenylimino)pent-2-en-2-ol) have been prepared and characterized by elemental analysis, NMR, FAB-mass, EPR, FT-IR, UV–Vis and cyclic voltammetry. The electronic structures and geometrical parameters of complexes **1** and **2** were analyzed by the theoretical B3LYP/DFT method. The interaction of these complexes **1** and **2** with CT-DNA has been explored by using absorption, cyclic voltammetric and CD spectral studies. From the electronic absorption spectral studies, it was found that the DNA binding constants of complexes **1** and **2** are 8.7×10^3 and 7.0×10^4 M^{-1}, respectively. From electrochemical studies, the ratio of DNA binding constants K_+/K_{2+} for **2** has been estimated to be >1. The high binding constant values, K_+/K_{2+} ratios more than unity and positive shift of voltammetric $E_{1/2}$ value on titration with DNA for complex **2** suggest that they bind more avidly with DNA than complex **1**. The inability to affect the conformational changes of DNA in the CD spectrum is the definite evidences of electrostatic binding by the complex **1**. It can be assumed that it is the bulky anthracene unit which sterically inhibits these complexes **1** and **2** from intercalation and thereby remains in the groove or electrostatic. The complex **2** hardly cleaves supercoiled pUC18 plasmid DNA in the presence of hydrogen peroxide. The results suggest that complex **2** bind to DNA through minor groove binding.

KEYWORDS
characterization, Cu(II) complexes, DNA binding, DNA cleavage, Schiff base ligands, theoretical studies

1 | INTRODUCTION

The interaction of transition metal complexes with DNA has been extensively studied in order to develop novel probes of DNA structure, DNA mediated electron transfer reactions and to find the potential biological and pharmaceutical activity. Their activity depends on the mode and affinity of the binding with DNA.[1–5] In

human blood plasma, the presence of transition metals reveals their importance in the living organisms as accumulated storage and transport. Transition metals play a key role in biological systems such as cell division, respiration, nitrogen fixation and photosynthesis.[6] Among the variety of ligand system employed in transition metal complexes, Schiff bases are an important class having many applications and many complexes of different Schiff bases have been reported by a number of authors.[7–12] Chelating Schiff base ligands containing O and N donor atoms show broad biological activity and are of special interest because of the variety of ways in which they are bound to metal ions.[13] Some of the Schiff base metal chelates shown the minor changes in the structure of the ligands containing hard soft donor atoms, markedly affects the activity of the compounds.[14] Schiff base complexes have received much attention as biomimics model compounds.[15] [Fe(salen)] complex is a model for natural iron protein, and hemerythrin has the ability to bind molecular oxygen reversibly.[16] Schiff base complexes incorporating two different metal ions are of special interest, as they are similar to those found in living organisms, like enzymes and proteins.[17] A large number of Schiff bases based metal complexes have been studied for their interesting and vital properties such as significant DNA binding ability, anticancer activity, catalytic activity in the hydrogenation of olefins, photochromic properties and so on.[18–23] Synthesis of new Schiff bases and their metal complexes are still pursued in many recent investigations.[24–26] Reddy *et al.* has synthesized ternary Cu(II) complexes of the type $[Cu(L')(L'')](ClO_4)$, where L'is N N-donor phenanthroline base and L' is an ancillary Schiff base ligand.[27] Schiff-base complexes have a wide variety of structures, coordinating to metal in either mono-, bi- and tri-dentate modes, depending upon the aldehyde and amines. Unsymmetrical Schiff-base ligand complexes have been suggested as useful biological models in understanding irregular binding of peptides and also as catalysts in some chemical processes.[11]

This paper deals with the preparation of new anthracene derived Schiff base ligands $\mathbf{L^1}$ and H($\mathbf{L^2}$) and their Cu(II) complexes $[Cu(\mathbf{L^1})Cl_2]$ (**1**), $[Cu(\mathbf{L^2})Cl]$ (**2**) and their characterizations using different elemental, spectroscopic and analytical tools. In addition to that, the structural parameters of complexes **1** and **2** were investigated by B3LYP/DFT studies. The DNA binding properties of complexes **1** and **2** have been studied with a view to evaluating their pharmaceutical activities. We believed that the complexes of **1** and **2** having anthracene derivative ligands, which possess planar aromatic moiety, are expected to bind strongly with DNA and to show promising chemotherapeutic activity.

2 | EXPERIMENTAL METHODS

2.1 | Materials

Anthracene-9-carbaldehyde, 1,2-diaminobenzene and acetylacetone were purchased from Alfa Aesar and used as received. Copper(II) chloride ($CuCl_2.\ 2H_2O$), calf thymus DNA and pUC18 plasmid DNA were obtained from Sigma Aldrich. All reagents and solvents were purchased from Merk and Loba chemie (India) and used without further purification.

2.2 | Physical measurements

UV–Vis spectra of solutions were recorded using Shimadzu spectrometer 2500 PC series. The FTIR spectra were recorded from KBr pellets in the range 400–4000 cm^{-1} on a Perkin-Elmer spectrometer. NMR spectra were obtained on a Bruker 300 MHz spectrometer. A mass analytical procedure was performed using a system consisting of a LC10ADVP pump and a single quadruple mass spectrometer with an electron spray ionization (ESI) source (LCMS-2010) (Shimadzu, Kyoto, Japan). Electron paramagnetic resonance (EPR) spectra were obtained using a Varian E-112 EPR spectrometer. CV measurements were carried out on Bio-Analytical System (BAS) model CV-50 W electrochemical analyser.

2.3 | Synthetic protocols

2.3.1 | N^1-(anthracene-9-methylene)benzene-1,2-diamine (L)

An ethanolic solution of anthracene-9-carbaldehyde (0.206 g, 1 mmol was added dropwise to a solution of 1, 2-diaminobenzene (0.108 g, 1 mmol dissolved in 20 ml of ethanol under constant stirring and the stirring was continued at room temperature for 6 h. After that, on slow evaporation of the solvent at room temperature, white shining precipitate was obtained. It was filtered, washed with petroleum-ether and recrystallized from ethanol. Yield: 88%.

2.3.2 | N^1,N^2-bis(anthracene-9-methylene) benzene-1,2-diamine (L^1)

An ethanolic solution of anthracene-9-carbaldehyde (0.412 g, 2 mmol) was added drop wise into a ethanolic solution of 1, 2-diaminobenzene (0.108 g, 1 mmol) with continuous stirring at room temperature. The resulting solution was refluxed for 3 h and the solvent was evaporated. The residue that formed was removed by filtration

and dried. The crude product was then recrystallized from ethanol. Yield: 82%.

2.3.3 | (2Z, 4E)-4-(2-(anthracen-9-ylmethyleneamino)phenylimino)pent-2-en-2-ol (H(L^2))

An ethanolic solution of acetylacetone (0.103 ML, 1 mmol) was slowly added to the ligand solution **L** (0.296 g, 1 mmol in 25 ml ethanol) under continuous stirring. The resulting mixtures was refluxed for 5 h and evaporated. The residue that formed was removed by filtration and the resulting solid was then recrystallized from ethanol. Yield: 70% The synthetic schemes for ligands **L**, $\mathbf{L^1}$ and H($\mathbf{L^2}$) are given in Scheme 1**.**

2.3.4 | [Cu(L^1)Cl_2] (1)

The ligand $\mathbf{L^1}$ (0.484 g, 1 mmol) was dissolved in 60 mL of absolute ethanol. An aqueous solution of 1 mmol of the $CuCl_2.2H_2O$ was added dropwise to the ligand solution with continuous stirring and refluxed for 5 h. The precipitate formed was filtered, washed with diethyl ether and recrystallized from ethanol.

2.3.5 | [Cu(L^2)Cl] (2)

The complex **2** was prepared using ligand H($\mathbf{L^2}$) (0.378 g, 1 mmol) by adopting the same synthetic procedure as given for complex **1**.

2.4 | Theoretical B3LYP/DFT studies

To get the electronic structure of the ground state complexes **1** and **2**, we carried out Density Functional Theory (DFT) analysis were executed by the hybrid exchange-correlation function with 6-31G (d,p) and B3LYP/LANL2DZ basis set using Gaussain 09 program.[28] Initially, the optimized geometries of the ligands ($\mathbf{L^1}$ and H($\mathbf{L^2}$)), complex **1** and **2** were obtained by the DFT-B3LYP program.

2.5 | DNA binding experiments

The DNA binding experiments were carried out using UV–visible absorption studies, cyclic voltammetry and circular dichroism studies.

2.6 | DNA cleavage study

The cleavage of pUC18 DNA by complexes **1** and **2**, in the absence and presence of activating agents H_2O_2 was demonstrated using agarose gel electrophoresis in 10% DMSO–5 mM Tris–HCl–50 mM NaCl buffer at pH 7.2.

3 | RESULTS AND DISCUSSION

Initially, complexes **1** and **2** were characterized by elemental analysis (Table 1). The elemental analyses result of the complexes **1** and **2** are in good agreement with their molecular formulas and the proposed chemical structure of the complexes **1** and **2** are depicted in **Figure** 1.

3.1 | ^{1}H and ^{13}C–NMR spectra

The ^{1}H and ^{13}C–NMR spectra of ligand $\mathbf{L^1}$ were recorded in $CDCl_3$, though **L** and H($\mathbf{L^2}$) were recorded in DMSO-d_6. The ^{1}H–NMR in addition to ^{13}C–NMR spectrum of **L** and $\mathbf{L^1}$ are shown in Figure S1 and S2, respectively. In the ^{1}H–NMR spectra, a sharp singlet

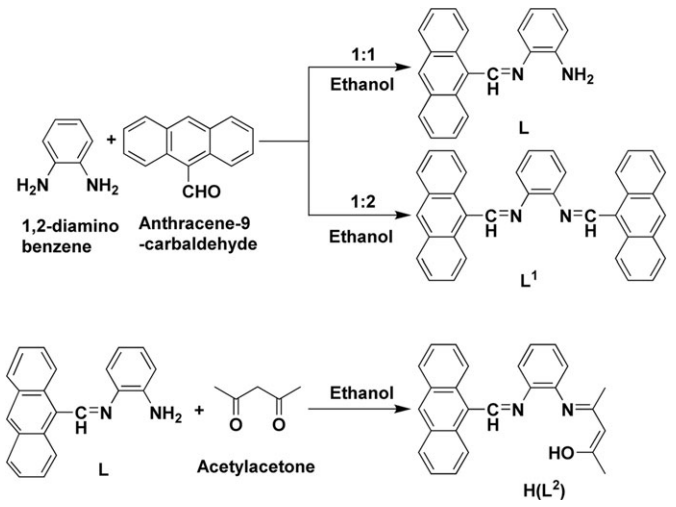

SCHEME 1 Schematic representation for the synthesis of ligands **L**, $\mathbf{L^1}$ and H($\mathbf{L^2}$)

TABLE 1 Elemental analysis and electronic spectral data of complexes **1** and **2**

	Found (Calcd)			λ_{max} (nm)		
Complex	**C**	**H**	**N**	**IL**	**LMCT**	**d-d**
1	69.76 (69.85)	3.93 (3.91)	4.44 (4.53)	255	377	915
2	66.15 (66.22)	4.41(4.49)	5.85 (5.94)	256	380	614

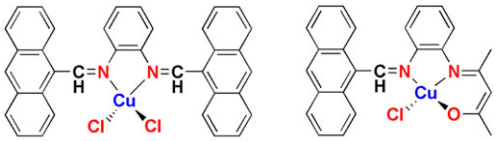

FIGURE 1 The proposed chemical structure of the complexes **1** and **2**

peak observed at δ, 8.99 (**L**) and 8.63 (**L**^{1}) ppm is due to = CH (azomethine) proton. The signal due to -OH proton of H(**L**^{2}) is observed at δ, 12.25 ppm and methyl protons appear in the range δ, 1.92–2.24 ppm. The aromatic protons are clustered at δ, (7.29–8.99 ppm). A broad signal at δ, 6.3 in the spectrum of **L** may be assigned to -NH_2 protons. The ^{13}C–NMR spectral data of ligands confirm the results obtained from the ^{1}H–NMR. The azomethine carbon atom (=CH) is observed at 149.78 ppm for **L**, 149.04 ppm for **L**^{1} and 156.02 ppm for H(**L**^{2}). Aromatic carbons are observed in the range δ, 113.46–156.02, 121.33–130.19 and 127.10–146.01 ppm for ligands **L**, **L**^{1} and H(**L**^{2}) respectively. The ^{13}C–NMR spectrum of H(**L**^{2}) exhibits –CH_3, −CH = C-CH_3, and = C-OH carbon resonance signals respectively at δ, 19.86–24.20, 95.26 and 176.16 ppm, correspondingly. As a result, the NMR spectral study well support with chemical structure of the ligands **L**, **L**^{1} and H(**L**^{2}).

3.2 | Mass spectra

The FAB-mass spectra of the complexes **1** and **2** show molecular ion peak consistent with the expected molecular weight and fragmentation pattern in accordance with the molecular formula. The FAB-mass spectrum of complex **1** shows molecular ion peak at $m/z = 620$ corresponding to its molecular weight. The other prominent peak at $m/z = 485$ may be due to **L**^{1}. The complex **2** (Figure S3) shows a molecular ion peak at $m/z = 496$ corresponding to its molecular weight. The other important peaks at $m/z = 441$ is due to loss of -Cl and at $m/z = 378$ corresponds to H(**L**^{2}). Thus, mass spectral analysis corroborates well with the proposed chemical structure of the complexes **1** and **2**.

3.3 | EPR spectral analysis

EPR spectra of the complexes **1** and **2** were recorded in DMSO solvent at liquid nitrogen temperature as well as at room temperature. At room temperature complexes **1** and **2** exhibit single derivative peak with the g values of 2.131 and 2.163, correspondingly. But, at liquid nitrogen temperature (77 K) the EPR spectra of the Cu(II) complex **1** exhibit a set of four well-resolved peaks in the low field region and a weaker signal in the high field region, corresponding to $g_{\parallel}$and $g_{\perp}$ respectively (Figure S4). The same trend was observed in complex **2** (Figure S5).

The $g_{\parallel}$and $g_{\perp}$ values are 2.245, 2.019 for **1** and 2.318, 2.015 for **2**, respectively. The trend observed as $g_{\parallel} > g_{\perp} > 2.02$, for the complexes **1** and **2** is typical of a Cu(II) ion (d^9) in axial symmetry with the unpaired electron present in the $d_{x^2-y^2}$ orbital.[29] It has been reported that $g_{\parallel}$values are close to 2.4 for the complexes containing copper–oxygen bonds and close to 2.3 for complexes containing copper–nitrogen bonds.[30] The complex **2** has the value of $g_{\parallel}$= 2.318 in conformity with the presence of both Cu–O and Cu–N bonds. The quotient ($g_{\parallel}$/ $A_{\parallel}$), which is empirically treated as a measure of the distortion from planarity, has been found to be 186 and 164 cm^{-1} for the complexes **1** and **2**, respectively indicating distortion from a square planar structure to a deformed tetrahedral structure.[31]

3.4 | FT-IR spectra

FT-IR spectra of free ligands **(L**, **L**^{1} and H(**L**^{2})**)**, complexes **1** and **2** were recorded using KBr disc and their characteristic bands are summarized in Table 2. The IR spectra of ligand **L**^{1} and complex **1** are shown in Figure S6. All the

TABLE 2 FT-IR spectral assignments of ligands (**L**, **L**^{1}, H(**L**^{2})), complexes **1** and **2** in cm^{-1}

Compound	**υ(O-H)**	**υ(C = N)**	**υ(M-N)**	**υ(M-O)**
L	-	1618	-	-
L^{1}	-	1621	-	-
H(**L**^{2})	3460	1624	-	-
1	-	1606	417	-
2	-	1606	415	560

ligands show a strong band in the range, 1624–1618 cm^{-1} due to azomethine (−C = N) stretching. These bands are shifted to lower frequencies, 1610–1589 cm^{-1} in the complexes, indicating coordination of the Schiff bases through the azomethine nitrogen.[32] The enolic υ(OH) band of the ligand H($\mathbf{L^2}$) observed at 3460 cm^{-1} disappeared upon complex formation with Cu(II), indicating the coordination of oxygen after deprotonation to the metal atoms. For complex **1**, the stretching vibration of υ(M-Cl) is observed below 350 cm^{-1} and not observed beyond 400 cm^{-1}. The coordination of the ligands $\mathbf{L^1}$ and H($\mathbf{L^2}$) to the metal through azomethine nitrogen and oxygen atom, after deprotonation, is further confirmed by the appearance of new bands around 431–417 and 560–545 cm^{-1} regions corresponding to υ(M-N) and υ(M-O) vibrational modes respectively.[33] The IR spectral data are in good agreement with the proposed structure for the complexes **1** and **2**. The broad absorption around 3480 cm^{-1} is due to water molecules present in the sample.

3.5 | Electronic absorption spectra

The electronic spectral data of complexes **1** and **2** associated structural assignments are given in Table 1. The UV- Vis spectra of these complexes **1** and **2** in DMSO exhibit a sharp absorption at 255 (**1**) & 256 (**2**) nm and a broad absorption at 377 (**1**) & 380 (**2**) nm owing to intra-ligand and ligand to metal charge transfer transitions, (LMCT) respectively (Figure S7). The very broad band's obtained in the region at 915 (**1**) & 614 (**2**) nm may be attributed to the d–d transition of Cu(II) ions.[34,35]

Broad and low energy bands are obtained for Cu(II) complexes **1** and **2** at 915 and 885 nm, respectively. It has already been reported that a lower energy transition can be observed between 730 and 900 nm, corresponding to the d–d transition.[36] This value is of particular importance since it was highly dependent on the geometry of the molecule. It is known that the transition from a square planar structure to a deformed tetrahedral structure leads to a red shift of absorption in the electronic spectrum.[37] Thus, the complexes **1** and **2**, are not perfectly square planar and the broad as well as low energy bands obtained at longer wavelengths are attributed to the deformed tetrahedral structure.

3.6 | Electrochemical behavior

Electrochemical data for the complexes **1** and **2** are summarized in Table 3 and their typical cyclic voltammetric responses are shown in Figure S8. Complexes **1** and **2** exhibit a quasi-reversible behavior as indicated by the non-equivalent current intensity at the cathodic and anodic peaks (i_{pa}/i_{pc} = 0.532–0.575). The peaks for the $Cu^{II/I}$ couple for the complexes **1** and **2** were observed in the potential range, + 0.400 V to – 0.400 V. The difference in peak potentials, ΔE_p = 0.131 (**1**) and 0.158 (**2**) V, exceeds the Nernstian requirement (0.059 V) suggesting that the complexes are quasi-reversible for electrochemical redox reactions.

TABLE 3 Voltammetric behavior* of complexes **1** and **2** in DMSO

Complex	E_{pc} (V)	E_{pa} (V)	ΔE_p (V)	i_{pc} (A)	i_{pa} (A)	i_{pa}/i_{pc}
1	0.012	0.143	0.131	1.15×10^{-5}	6.12×10^{-6}	0.532
2	0.011	0.169	0.158	1.19×10^{-5}	6.23×10^{-6}	0.575

*Measured vs Ag/AgCl with TBAP as supporting electrolyte at 100 mVs^{-1}.

3.7 | The ground state structures by theoretical DFT calculation

Density functional theory (DFT) calculations were used to investigate the mode of complex formation; electronic structures as well as geometrical parameters of complexes **1** and **2**, as their crystal structure have not been obtained. The structure of complexes **1** and **2** in the gas phase was determined to be Cu(II) centered complexes with distorted tetrahedral geometry and the optimized structures of complexes **1** and **2** are depicted in Figure 2. These structures of complexes **1** and **2** are well correlated with the results of spectroscopic and analytical investigations.

Further, the Frontier molecular orbital structures of ligands ($\mathbf{L^1}$ and H($\mathbf{L^2}$)), complex **1** and **2** are displayed in Figure 3 and 4, respectively. In $\mathbf{L^1}$, HOMO is spread over the whole π-moiety and LUMO on the anthracene unit. After complexation with Cu(II) (complex **1**) HOMO of $\mathbf{L^1}$ is localized on the part of the π-moiety and more spread in metal part and the same behavior is observed as $\mathbf{L^1}$-LUMO with little contribution of metal ion. Similarly for H($\mathbf{L^2}$), HOMO and LUMO spread over the whole π-moiety. Then, HOMO is spread on imine and metal parts and LUMO is spread over the whole molecular frame structure after complex **2** formations. Moreover, the calculated HOMO-LUMO energy gaps of $\mathbf{L^1}$ and H($\mathbf{L^2}$) are 2.82 eV and 2.97 eV, respectively. After complexation with Cu^{2+}, the HOMO-LUMO energy gaps of complex **1** and **2** are found to be 1.76 eV and 2.33 eV. These results obviously indicate that the complexation of ligands $\mathbf{L^1}$ and H($\mathbf{L^2}$) with Cu^{2+}, resulting in the disruption of the internal charge transfer and that resulted in the changes in electronic properties.

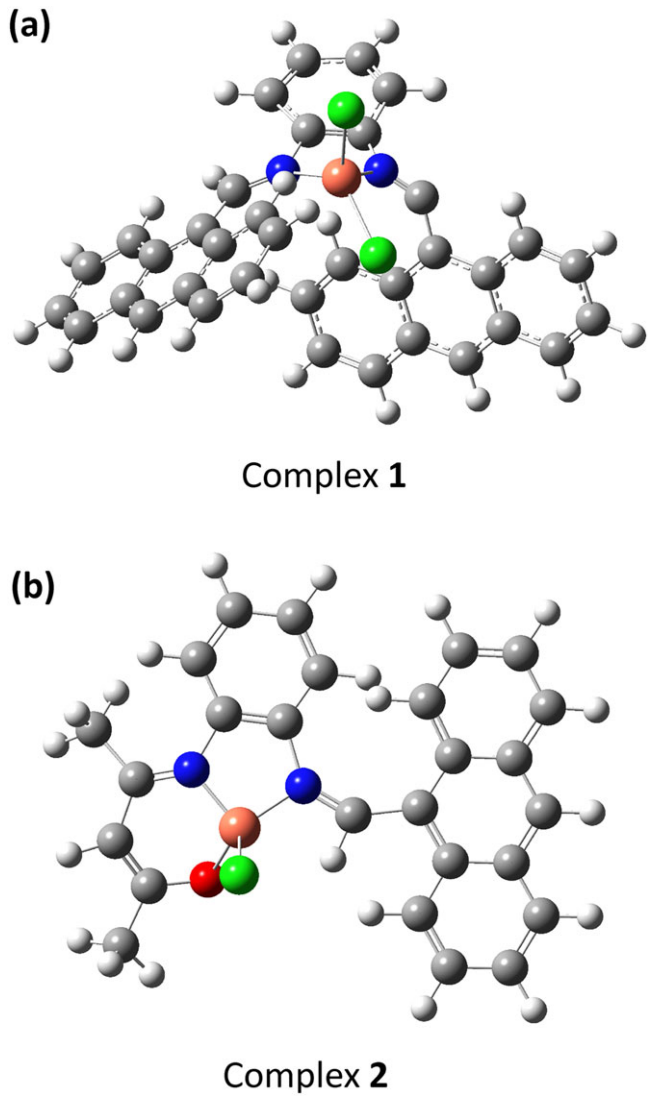

FIGURE 2 Gas phase B3LYP/DFT optimized structure of complexes **1** and **2**

3.8 | DNA binding and cleavage studies

3.8.1 | Absorption spectroscopic titration

Absorption titration experiments were performed by maintaining the Cu(II) complexes **1** and **2** concentration as constant at 20 μM while varying the concentration of CT-DNA in between 0–100 μM. Table 4 summarizes the spectral changes when the complexes **1** and **2** are titrated with DNA. LMCT bands (377 nm (**1**) – 380 nm (**2**)) are monitored for absorption spectroscopic titration. Addition of increasing amounts of DNA results in hypochromism and a moderate bathochromic shift (2–4 nm) of the peak at the LMCT band. The absorption spectra of complexes **1** and **2** in the presence of increasing amounts of DNA are shown in Figure 5.

For complex **1**, LMCT absorption (377 nm) shifts up to only 2 nm with 14–18% hypochromism. As for complex **2** the intensity of the LMCT band at (380 nm) markedly decreased in presence of DNA, 23–34% hypochromism, with a red shift up to 4 nm. The binding constant of complex **2** has been found to be 7.0×10^4 M^{-1} and this values are higher than that obtained for complex **1** (8.7×10^3 M^{-1}). The intrinsic binding constant values obtained for **1** and **2** are lower than that of potential intercalator like ethidium bromide ($K_b = 7.0 \times 10^7$ M^{-1})[38], but comparable to those observed for $[Cu(phen)_2]^+$ and $[Ru(phen)_3]^{2+}$.[39]

From the absorption titration results, it could be seen that the spectral changes for the complexes **1** and **2** are not uniform. The spectral characteristic of low hypochromism, paltry red shift and low K_b values observed for the complex **1** suggest that there is no likelihood of intercalative binding to DNA due to two bulky anthracene units which strongly prevent stacking the aromatic chromophore between the base pairs of the DNA. The high K_b values and pronounced hypochromism for complex **2** are possibly due to the presence of only one anthracene moiety that facilitates groove binding with the DNA with the base pairs.[40] Taking into account the extent of hypochromism and binding constant values the possibility of intercalative binding of DNA can be ruled out and only groove binding may occur for complexes **1** and **2**.

3.8.2 | Electrochemical studies

Electrochemical investigation of drug–DNA interactions can provide a useful complement to other methods and yield information about the mechanism of interaction and the conformation of adduct.[41] The electrochemical behavior of complexes **1** and **2**, and their interaction with CT-DNA were carried out by CV. The cyclic voltammetric data for complexes **1** and **2** in the absence and presence of DNA at room temperature in Tris–HCl buffer (pH = 7.1) is shown in Table 5.

The cyclic voltammogram of complex **1** in the absence of DNA reveals reduction of Cu^{II} to the Cu^{I} form at a cathodic peak potential (E_{pc}) of −0.010 V *versus* Ag/AgCl. In the absence of DNA, the separation of the anodic and cathodic peak potentials, $\Delta E_p = 0.093$ V for **1** indicates a quasi-reversible redox process. The formal potential, $E_{1/2}$ (or voltammetric $E_{1/2}$), taken as the average of E_{pc} and E_{pa} is 0.037 V in the absence of DNA. The presence of DNA in the solution at the same concentration of complex causes a considerable decrease in the voltammetric current. In addition, both the peak potentials, (E_{pc} and E_{pa}) and $E_{1/2}$ have shifted to more negative potential/less positive as shown in Figure 6.

The cyclic voltammogram of complex **2** in the absence of DNA features a quasi-reversible redox wave with

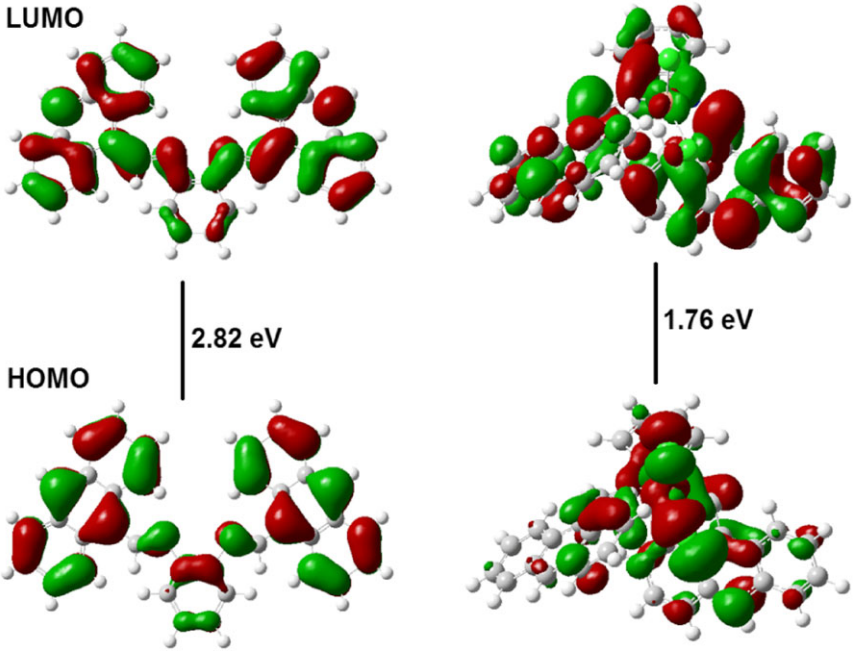

FIGURE 3 Frontier molecular orbitals of $\mathbf{L^1}$ and complex **1** (from left to right)

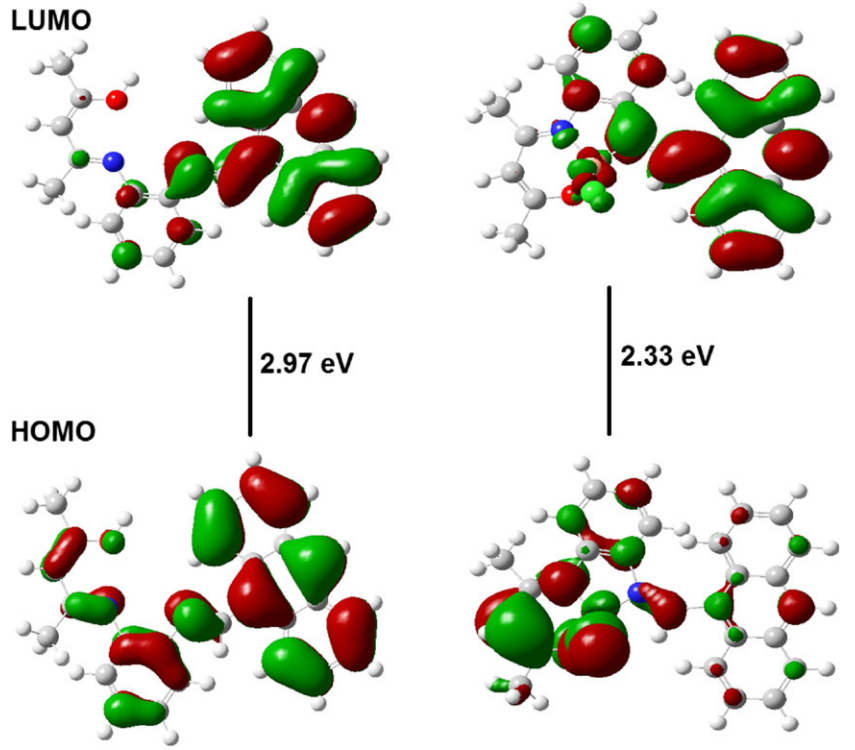

FIGURE 4 Frontier molecular orbitals of H($\mathbf{L^2}$) and complex **2** (from left to right)

TABLE 4 Absorption spectral titration data of the complexes **1** and **2** with DNA in Tris–HCl buffer solution

Complex	LMCT (λ_{max}/nm)		Hypochromism (%)	Red shift Δ λ (nm)	Binding constant K_b (M^{-1})
	Free	Bound			
1	377	379	14–18	2	8.7×10^3
2	380	384	23–34	4	7.0×10^4

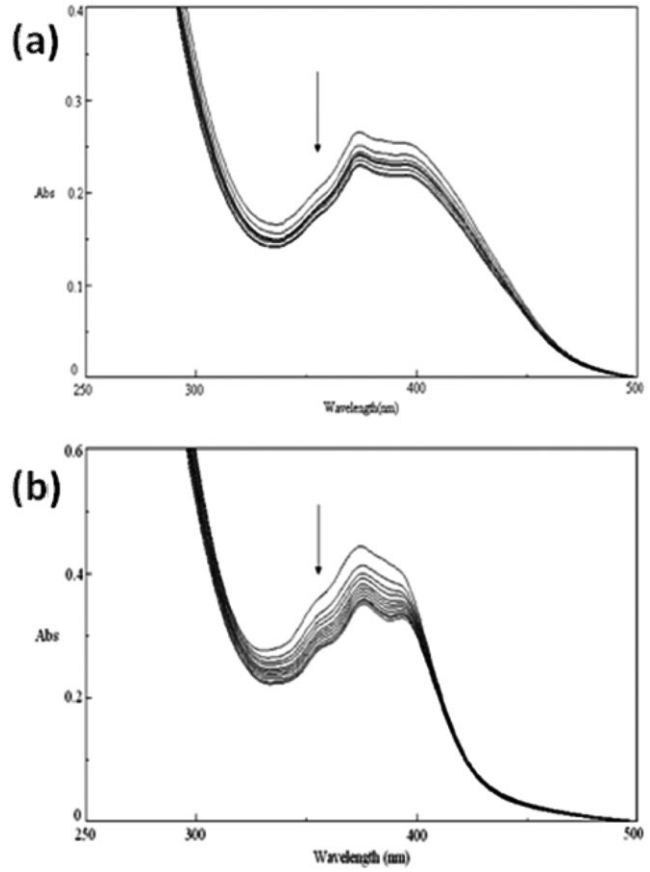

FIGURE 5 Absorption spectra of complex **1** (a) and **2** (b) in the absence and presence of increasing amounts of DNA (0–240 μM) in Tris–HCl buffer (pH = 7.1). Arrow mark indicates the absorbance change upon increasing DNA concentration. [complex] = 20 μM

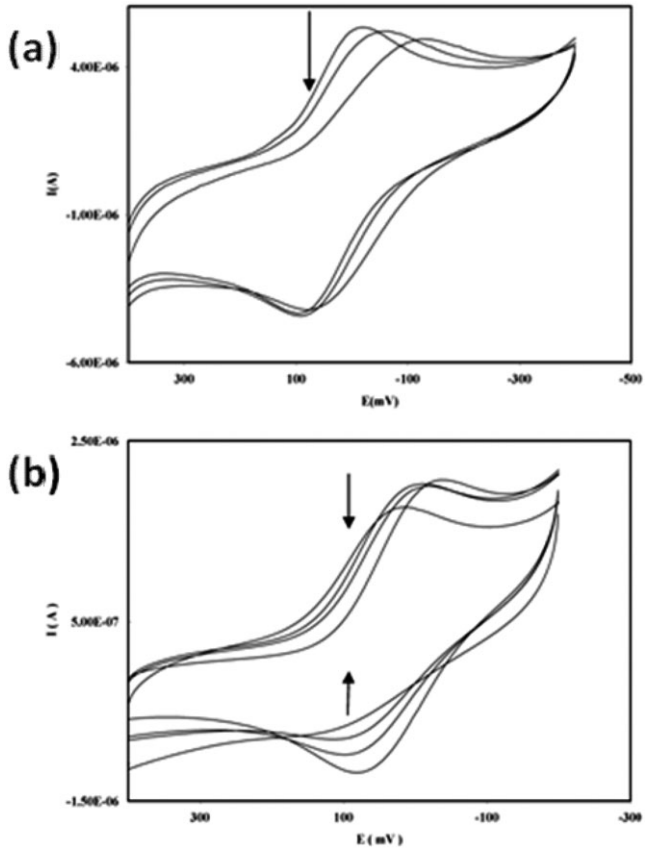

FIGURE 6 Cyclic voltammograms of **1** (a) and **2** (b) in the absence and in presence of DNA in Tris–HCl buffer pH = 7.1. [complex] = 100 μM. [R = 0, 4 & 8]

TABLE 5 Voltammetric behavior of complexes **1** and **2** towards DNA in Tris–HCl buffer solution

Complex	R	E_{pc} (V)	E_{pa} (V)	ΔE_p (V)	i_{pa}/i_{pc}	$E_{1/2}$ (V)	$\Delta E_{1/2}$ (V)	K_+/K_{2+}
1	0	−0.010	0.083	0.093	0.972	0.037		
	4	−0.044	0.077	0.121	1.129	0.017	−0.020	0.46
	8	−0.102	0.051	0.153	1.057	−0.026	−0.063	0.12
2	0	−0.035	0.083	0.118	0.400	0.006		
	4	−0.077	0.074	0.151	0.526	0.017	−0.029	2.10
	8	−0.114	0.051	0.165	0.983	−0.034	−0.080	7.43

E_{pc} = −0.035 V at a scan rate of 100 mVs^{-1} and the measured half wave potential $E_{1/2}$ for the Cu(II)/(I) couple is 0.006 V. The ratio of anodic to cathodic peak current is 0.4 which closely resembles that of the criteria of quasi-reversibility. Upon addition of increasing amounts of DNA the cyclic voltammogram of the complex **2** experienced a less negative shift in cathodic peak potential and more positive shift in both the anodic peak potential and voltammetric $E_{1/2}$ at the same scan rate. After the addition of DNA, $E_{1/2}$ is shifted to −0.034 V, ΔEp is 0.080 V and i_{pa}/i_{pc} value is increased to 0.526.

The drop in the voltammetric current in the presence of DNA in complexes **1** and **2** can be attributed to the diffusion of the Cu(II) complex bound to the large, slowly diffusing DNA molecule. In the cyclic voltammograms of **1** and **2**, at different concentrations of DNA, the peak currents decreased with increasing concentrations of DNA while both the Epc and E'^0 shifted to more positive or less negative potentials. The phenomena of the shift of E'^0 and the decrease of peak current implied forming a new association of DNA with complex. Based on the shift of formal potentials in the cyclic voltammograms, the interaction mode of compounds with DNA can be inferred.[42] Therefore, in the light of Bard's report,[43] complex **2** may interact with DNA by groove binding mode in contrast to **1** whose interaction mode is electrostatic due to negative shift of E'^0 in these cases. For complex **1,** K_{2+} is higher than K_+ while the reverse is observed for the complex **2**. This suggests that the B form of DNA tends to stabilize the Cu(II) over the Cu(I) state of the complex **1** obviously by electrostatic interaction and

thereby indicating that the species Cu(II) interacts with DNA to a greater extent than Cu(I). In short, the obvious shift of peak potentials and the ratio of binding constant values suggest a weak association of the complex **1** ($K_+/K_{2+} < 1$) with DNA than complex **2** ($K_+/K_{2+} > 1$).

3.8.3 | Circular dichroism study

The results of CD studies for **1** and **2** are presented in Figure 7. Pure DNA produced characteristic bands with a positive band at 278 nm and a negative band at 244 nm. These bands were modified when DNA was allowed to interact with complexes **1** and **2**.

In presence of complex **1**, the intensity of the negative ellipticity band decreases almost similar to that for the positive ellipticity band. This suggests that the DNA-binding of the complexes do not affect the conformational changes of DNA. Furthermore, with increasing concentration of complex **1**, it proved difficult to detect any obvious perturbation in the CD spectrum; illustrating the inability of complexes to affect the conformational heterogeneity of DNA anymore.[44]

In presence of complex **2** an increase in the molar ellipticity values of both the positive and negative ellipticity bands of the DNA was observed, consistent with a single binding mode. The enhancement of the intensity of positive band along with a minor red shift (Figure 7) of the band maxima is characteristic of groove binding that stabilizes right-handed B form of DNA.[45] The CD spectral studies suggest that while the DNA binding of complex **1** involves electrostatic mode, complex **2** wraps the groove of the DNA. These conclusions are also in accordance with those from electronic spectral and cyclic voltammetric studies.

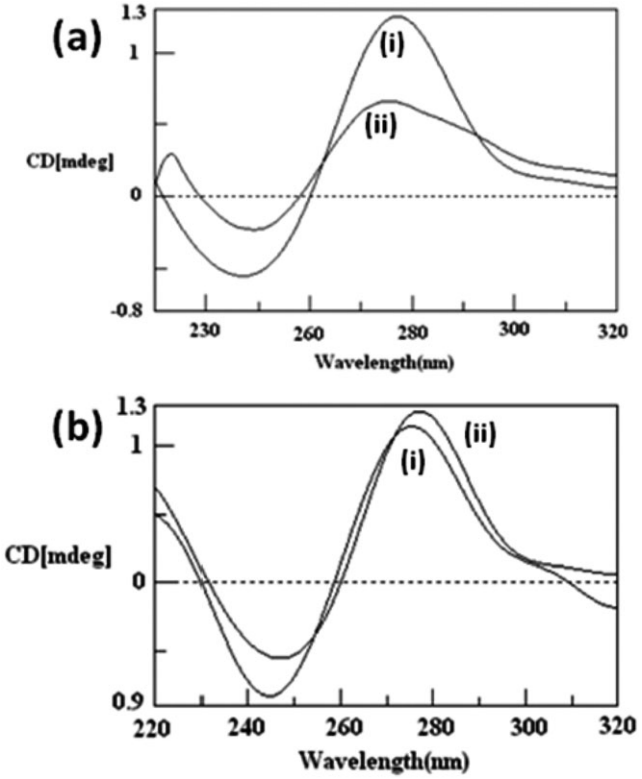

FIGURE 7 CD spectra of CT- DNA in the absence (i) and presence (ii) of complex **1** (a) and complex **2** (b); [DNA] = 200 μM, [complex] = 100 μM, ($1/R = 0.5$)

3.8.4 | DNA cleavage study by gel electrophoresis

Based on the above investigation, Complex **2** has potent DNA binding ability than complex **1** and it needs to probe the DNA cleavage characteristics of complex **2** for fulfilling the basic requirements as an anticancer agent.

Figure 8 illustrates the gel electrophoretic separations showing the cleavage of plasmid pUC18 DNA induced by the complex **2** under aerobic conditions. With the increase of complex concentration, no amount of the circular supercoiled DNA is converted into nicked DNA *via* single strand cleavage (lane 4). It reveals that pUC18 DNA induced by the complex in the presence of high concentration of H_2O_2 results in the insignificantly small conversion of Form I to Form II (lane 6). H_2O_2 alone is incapable of cleaving plasmid DNA (lane 3). It can be seen that neither the complex **2** alone nor incubation with H_2O_2 without the complex causes any strand scission (lanes 2 and 3). These experiments demonstrate that both the copper(II) complex and high amount of H_2O_2 are required

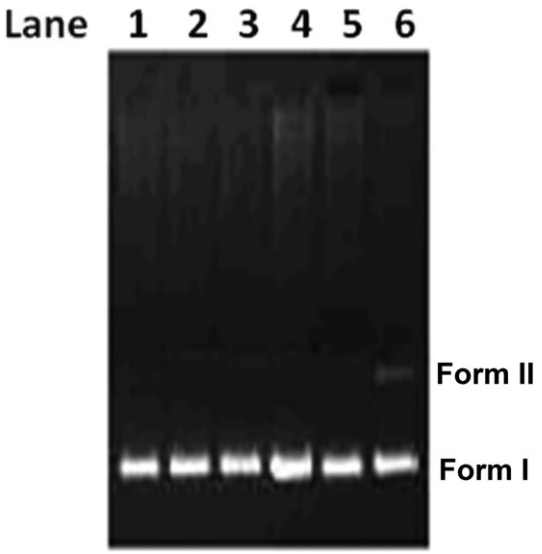

FIGURE 8 Agarose gel electrophoresis diagram showing the cleavage of SC pUC18 DNA (500 ng) by complex **2** in Tris–HCl/NaCl buffer (50 mM, pH = 7.2) lane 1, DNA control; lane 2, Lane1 + 50 μM complex; lane 3, Lane1 + 100 μM H_2O_2; lane 4, lane 1 + 100 μM complex; lane 5, lane 1 + 100 μM complex +100 μM H_2O_2; Lane6, lane 1+ 100 μM complex +200 μM H_2O_2

to cleave plasmid DNA even to very small extent. The inability of the complex **2** to cleave plasmid pUC18 DNA can be attributed to the ratio K_+/K_{2+}, obtained from CV studies, which is less than unity. To have an observable nuclease activity the ratio K_+/K_{2+} should be >1.[46,47] The cleavage mechanism may involve a hydroxyl radical oxidative mechanism.

4 | CONCLUSION

In summary, new anthracene based Schiff base ligands $\mathbf{L^1}$ and H($\mathbf{L^2}$) and their derived Cu(II) complexes **1** and **2** have been synthesised and well characterized by using various spectroscopic and analytical methods. The molecular structures of the Cu(II) complexes **1** and **2** were ascertained by a theoretical method (B3LYP/DFT analysis). *In vitro* DNA binding studies have been performed using various biophysical techniques *viz.,* absorption, cyclic voltammetry, and circular dichroism techniques, to predict their binding mode as well as binding strength; the results revealed higher binding affinity of complex **2** than complex **1**, *via* groove mode of binding. For the reason that, complex **1** has a bulkier in size than complex **2**, which make the barrier to bind with DNA *via* groove mode of interaction. However, complex **1** showed significant binding ability through electrostatic interaction with DNA helix. We also analyzed the pUC18 DNA cleavage capability of complex **2**, which gives oxidative pathways chase cleavage pattern. These results fortify our idea of minor groove binding nature of complex **2** with DNA. In conclusion, we believe that these Cu(II) complexes are alternatives as better anticancer agents and additional studies are needed on complex **2**, to recommend as a cancer drug in preclinical study.

ACKNOWLEDGEMENTS

This work was supported by the DST-SERB (Grant. No: SB/FT/CS-130/2012). We express our gratitude to Madurai Kamaraj University and Mohamed Sathak Engineering College, Kilakarai for their lab facilities and their instrumentation facilities.

ORCID

Jegathalaprathaban Rajesh http://orcid.org/0000-0001-6118-7049

REFERENCES

[1] R. Indumathy, S. Radhika, M. Kanthimathi, T. Weyhermuller, B. Unni Nair, *J. Inorg. Biochem.* **2007**, *101*, 434.

[2] L. Li, K. D. Karlin, S. E. Rokita, *J. Am. Chem. Soc.* **2005**, *127*, 520.

[3] A. Silvestri, G. Barone, G. Ruisi, M. Giudice, S. Tumminello, *J. Inorg. Biochem.* **2004**, *98*, 589.

[4] N. Nagesh, G. Raju, R. Srinivas, P. Ramesh, M. D. Reddy, C. R. Reddy, *Biochim. Biophys. Acta* **2015**, *1850*, 129.

[5] G. Raju, R. Srinivas, M. D. Reddy, C. R. Reddy, N. Nagesh, *Nucleos. Nucleot. Nucl. Acids.* **2014**, *33*, 489.

[6] J. D. Joshi, S. Sharma, G. Patel, J. J. Vora, *Synth. React. Inorg. Met-Org.Chem.* **2002**, *31*, 1729.

[7] M. S. Surendra Babu, K. Hussain Reddy, P. G. Krishna, *Polyhedron* **2007**, *26*, 572.

[8] C. Tu, X. Wu, Q. Liu, X. Wang, Q. Xu, Z. Guo, *Inorg. Chim. Acta* **2004**, *357*, 95.

[9] A. Terenzi, R. Bonsignore, A. Spinello, C. Gentile, A. Martorana, C. Ducani, B. Högberg, A. M. Almerico, A. Lauria, G. Barone, *RSC Adv.* **2014**, *4*, 33245.

[10] A. Mederos, S. Dominguez, R. Hernandez-Molina, J. Sanchiz, F. Brito, *Coord. Chem. Rev.* **1999**, *193*, 857.

[11] D. M. Boghaei, S. Mohebi, *Tetrahedron* **2002**, *58*, 5357.

[12] M. S. Islam, M. A. Farooque, M. A. K. Bodruddoza, *Synth. React. Inorg. Met. Org. Chem.* **2002**, *32*, 1811.

[13] R. C. Maurya, P. Patel, S. Rajput, *Synth. React. Inorg. Met.-Org. Chem.* **2003**, *33*, 817.

[14] N. Deligönül, M. Tümer, S. Serin, *Transit. Metal. Chem.* **2006**, *31*, 920.

[15] M. Tyagi, S. Chandra, J. Akhtar, D. Chand, *Spectrochim. Acta A Mol. Biomol. Spectrosc.* **2014**, *118*, 1056.

[16] T. P. Ribeiro, C. Fernandes, K. V. Melo, S. S. Ferreira, J. A. Lessa, R. W. A. Franco, G. Schenk, M. D. Pereira, A. Horn, *Free Radical Biol. Med.* **2015**, *80*, 67.

[17] J. A. Prescher, C. R. Bertozzi, *Nat. Chem. Biol.* **2005**, *1*, 13.

[18] A. H. Osman, *Trans. Met. Chem.* **2006**, *31*, 35.

[19] S. M. Abdallah, M. A. Zayed, G. G. Mohamed, *Arab. J. Chem.* **2010**, *3*, 103.

[20] L. Chen, Y. Xiang, T. Feng, *Appl. Organomet. Chem.* **2012**, *26*, 108.

[21] P. Kavitha, M. Rama Chary, B. V. V. A. Singavarapu, K. Laxma Reddy, J. Saudi, *Chem. Soc.* **2016**, *20*, 69.

[22] A. Gubendran, M. P. Kesavan, S. Ayyanaar, J. Dhaveethu Raja, P. R. Athappan, J. Rajesh, *Appl. Organomet. Chem.* **2017**, e3708. https://doi.org/10.1002/aoc.370834.

[23] M. Damoder Reddy, E. Blake Watkins, *J. Org. Chem.* **2015**, *80*, 11447.

[24] A. Golcu, M. Tumer, H. Demicell, R. C. Wheatley, *Inorg. Chim. Acta* **2005**, *358*, 1785.

[25] P. G. Lacroix, F. Averseng, I. Malfant, K. Nakatani, *Inorg. Chim. Acta* **2004**, *357*, 3825.

[26] S. Dhar, M. Nethaji, A. R. Chakravarty, *Inorg. Chim. Acta* **2005**, *358*, 2437.

[27] P. A. N. Reddy, B. K. Santra, M. Nethaji, A. R. Chakravarty, *J. Inorg. Biochem.* **2004**, *98*, 377.

[28] M. J. Frisch, G. W. Trucks, H. B. Schlegel, G. E. Scuseria, M. A. Robb, J. R. Cheeseman, G. Scalmani, V. Barone, B. Mennucci, G. A. Petersson, H. Nakatsuji, M. Caricato, X. Li, H. P. Hratchian, A. F. Izmaylov, J. Bloino, G. Zheng, J. L. Sonnenberg, M. Hada, M. Ehara, K. Toyota, R. Fukuda, J. Hasegawa, M. Ishida, T. Nakajima, Y. Honda, O. Kitao, H. Nakai, T. Vreven, J. A. Montgomery, Jr., J. E. Peralta, F. Ogliaro, M. Bearpark, J. J. Heyd, E. Brothers, K. N. Kudin, V. N. Staroverov, R. Kobayashi, J. Normand, K. Raghavachari, A. Rendell, J. C. Burant, S. S. Iyengar, J. Tomasi, M. Cossi, N. Rega, J. M. Millam, M. Klene, J. E. Knox, J. B. Cross, V. Bakken, C. Adamo, J. Jaramillo, R. Gomperts, R. E. Stratmann, O. Yazyev, A. J. Austin, R. Cammi, C. Pomelli, J. W. Ochterski, R. L. Martin, K. Morokuma, V. G. Zakrzewski, G. A. Voth, P. Salvador, J. J. Dannenberg, S. Dapprich, A. D. Daniels, O. Farkas, J. B. Foresman, J. V. Ortiz, J. Cioslowski, D. J. Fox, Gaussian, Inc., Wallingford, CT, **2009**.

[29] N. M. El-Metwally, I. M. Gabr, A. A. Asmy, A. A. Abou-Hussen, *Trans. Met. Chem.* **2006**, *31*, 71.

[30] M. Massacesi, D. G. Ponticelli, V. B. Addepalli, V. G. Krishnan, *J. Mol. Struct.* **1979**, *51*, 27.

[31] M. P. Kesavan, G. G. Vinoth Kumar, J. Dhaveethu Raja, K. Anitha, S. Karthikeyan, J. Rajesh, *J. Photochem. Photobio. B: Bio.* **2017**, *167*, 20.

[32] R. Ramesh, P. K. Suganthy, K. Natarajan, *Synth. React. Inorg. Met.-Org. Chem.* **1996**, *26*, 47.

[33] P. Tyagi, S. Chandra, B. S. Saraswat, D. Sharma, *Spectrochim. Acta A Mol. Biomol. Spectrosc.* **2015**, *143*, 1.

[34] R. G. McDanald, M. I. Riley, M. A. Hitchman, *Inorg. Chem.* **1989**, *28*, 752.

[35] A. B. P. Lever, *Inorganic Electronic Spectroscopy*, Elsevier, Amsterdam **1984**.

[36] L. Nivorozhkin, H. Toflund, P. L. Jorgensen, L. E. Nivorozhkin, *J. Chem. Soc., Dalton Trans.* **1996**, *7*, 1215.

[37] K. H. Kumar Naik, S. Selvaraj, N. Naik, *Spectrochim. Acta A Mol. Biomol. Spectrosc.* **2014**, *131*, 599.

[38] P. Tamil Selvi, M. Palaniandavar, *Inorg. Chemica. Acta.* **2002**, *337*, 420.

[39] M. Navarro, *J. Inorg. Biochem.* **2003**, *97*, 364.

[40] K. Dhara, J. Ratha, M. Manassero, X. Y. Wang, S. Gao, P. Banerjee, *J. Inorg. Biochem.* **2007**, *101*, 95.

[41] M. S. Ibrahim, *Anal. Chim. Acta* **2001**, *443*, 63.

[42] X. Lu, K. Zhu, M. Zhang, H. Liu, J. Kang, *J. Biochem. Biophys. Methods* **2002**, *52*, 189.

[43] S. S. Zhang, S. Y. Niu, B. Qu, G. F. Jie, H. Xu, C.-F. Ding, *J. Inorg. Biochem.* **2005**, *99*, 2340.

[44] P. Uma Maheswari, M. Palaniandavar, *J. Inorg. Biochem.* **2003**, *98*, 219.

[45] A. K. Patra, M. Nethaji, A. R. Chakravarty, *J. Inorg. Biochem.* **2007**, *101*, 233.

[46] P. Zhang, P. J. Sadler, *Eur. J. Inorg. Chem.* **2017**, *12*, 1541.

[47] S. Mahadevan, M. Palaniandavar, *Inorg. Chem.* **1998**, *37*, 3927.

SUPPORTING INFORMATION

Additional Supporting Information may be found online in the supporting information tab for this article.

How to cite this article: Gubendran A, Kumar GGV, Kesavan MP, Rajagopal G, Athappan P, Rajesh J. New anthracene based Schiff base ligands appended Cu(II) complexes: Theoretical study, DNA binding and cleavage activities. *Appl Organometal Chem*. 2017;e4128. https://doi.org/10.1002/aoc.4128